ICAS 2016

30th Congress of the International Council
of the Aeronautical Sciences
DCC, Daejeon, Korea; September 25 - 30, 2016

INFLUENCE OF THE RHOMBOID ZONE ON AEROELASTIC EXPERIMENTS OF SUPERSONIC AIRCRAFT

Yuguang Bai*, Wei Qian*
***School of Aeronautics and Astronautics, Faculty of Vehicle Engineering and Mechanics, Dalian University of Technology, Dalian 116023, China**
Keywords: *aeroelastic experiment; CFD; rhomboid zone; DES; supersonic aircraft*

Abstract

When a scaled flutter model is designed for aeroelastic experiment in a specific wind tunnel, the size of it was recognized to be installed within the rhomboid zone. This paper discussed the influence of the rhomboid zone of a wind tunnel on aeroelastic experiment for supersonic aircraft. Three sizes of flutter models of a same aircraft structure were modelled with structure-similarity and the exceed range outside the rhomboid of them were different. Aerodynamic force and Flow distributions around the three models were predicted with engineering algorithm and CFD method. Detached eddy simulation, which can obtain a good balance between calculated expense and accuracy, was adopted for three dimensional turbulence computation. Then their aeroelastic characteristic were compared. It was found from the compared results that when the model size exceed a range, flow distribution can provide a significant influence on the experimental results for a flutter model of supersonic aircraft. Inversely, the influence can be neglected if the exceed range do not cause serious changes of flow distribution around the model.

1. Introduction

Wind tunnel experiment is one of the most effective way to test flutter characteristics of supersonic aircraft. Due to consideration of frequency similarity and the limit of the frequency ratio of a wind tunnel, the scaled ratio is limited. So the size of a scaled model cannot be determined arbitrarily small. If the scaled model is installed beyond the rhomboid zone of a wind tunnel, the flow field around the model will not be uniform. It means that influence on the experimental results due to the inconsistency of flow must be evaluated. This paper discussed this influence and proposed an exceed range of the sample wind tunnel in which the influence can be neglect.

During the discussion process, an effective numerical method should be adopted. This paper used engineering algorithm and CFD method to provide the basis of numerical computation. This methodology can be a useful reference for evaluation of wind tunnel experiments.

2. Rhomboid zone

The concept of rhomboid zone was proposed based on the principle of shock wave [1] (i.e. when the model is installed inside rhomboid zone, the flow field is not influence by jump due to the rear of the model. Fig.1 is the sample of rhomboid zone of a wind tunnel in China.

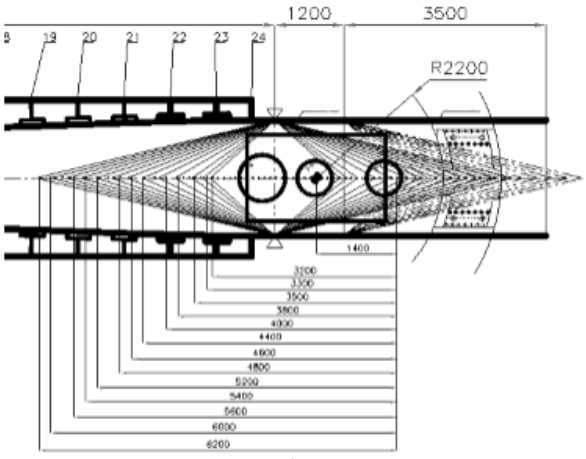

Fig.1 Rhomboid zone of a wind tunnel in China.

The length of rhomboid zone is

$$L \le 0.7L_1 = 0.7H\sqrt{Ma^2 - 1} \qquad (1)$$

where L is the length of rhomboid zone; H is the height of the wind tunnel; Ma is Mach number; and L_1 is the length of the first rhomboid zone.

3. Numerical method

3.1 Engineering algorithm

$$C_p = \begin{cases} \left[1/(\sin(4\delta)^{\frac{3}{4}}) + 1\right]\sin^2\delta, & \delta \le 22.5° \\ 2\sin^2\delta, & \delta \le 22.5° \end{cases} \quad (2)$$

A modified Dahlem-Buck equation was used [2]. The parameter δ represents angle of impact.

3.2 CFD method

This paper employed detached eddy simulation [3] to provide accurate results when computational expense was acceptable.

The present numerical method combined the advantage of Menter's two equation mode and Shur's IDDES mode:

$$\frac{\partial}{\partial t}(rk)+\frac{\partial}{\partial x_i}(rU_j k) = t_{ij}S_{ij}+\frac{\partial}{\partial x_j}\left[(m+s_k m_t)\frac{\partial k}{\partial x_j}\right]-\frac{rk^{1.5}}{l_{hybrid}} \quad (3)$$

here $l_{hybrid} = \min\left(\frac{l_{LES}}{1-F_{SST}}, l_{RANS}\right)$; $m_{t,zonal} = (rC_{DES}k^{1/2}\Delta)$; and $F_{SST} = \begin{cases} F_1 \\ F_2 \end{cases}$. This method introduce a hybrid function F_{SST}, which can coupling dissipative terms and eddy viscosity coefficients of near wall and far wall. Besides, there is:

$$l_{DDES} = l_{RANS} - f_d \max(0, l_{RANS} - l_{LES}) \quad (4)$$

and Shur et al. proposed that

$$l_{IDDES} = \tilde{f}_d(1+f_e)l_{RANS} + (1-\tilde{f}_d)l_{LES} \quad (5)$$

In the present paper, CFD method was adopted by the commercial software ANSYS CFX.

3.3 Fundamentals of Aeroelasticity

Aeroelastic response of flight vehicle is a result of the mutual interaction of inertial and elastic structural forces, aerodynamic forces induced by the static or dynamic deformation of the structure, and external disturbance forces. The equation of motion of the aeroelastic system in terms of discrete system can be derived based on the equilibrium condition of these forces [4], i.e.:

$$\overline{\mathbf{M}}\ddot{\mathbf{x}}(t) + \overline{\mathbf{K}}\,\mathbf{x}(t) = \mathbf{F}(t) \quad (6)$$

Where $\overline{\mathbf{M}}$ and $\overline{\mathbf{K}}$ are the mass and stiffness matrices generated by the structural finite element method. $\mathbf{x}(t)$ is the structural deformation.

$\mathbf{F}(t)$ can be generally split into two parts; the aerodynamic forces induced by the structural deformation $\mathbf{F}_a(\mathbf{x})$ and the external forces $\mathbf{F}_e(t)$, i.e.:

$$\mathbf{F}(t) = \mathbf{F}_a(\mathbf{x}) + \mathbf{F}_e(t) \quad (7)$$

The external forces $\mathbf{F}_e(t)$ are usually provided. Typical example of $\mathbf{F}_e(t)$ is the continuous atmospheric turbulence, impulsive-type gusts, store ejection forces or control surface aerodynamic forces due to pilot's input command. The generation of $\mathbf{F}_a(\mathbf{x})$ normally relies on the theoretical prediction that requires the unsteady aerodynamic computations. Since $\mathbf{F}_a(\mathbf{x})$ depends on the structural deformation $\mathbf{x}(t)$, the relationship can be interpreted as an aerodynamic feedback. Fig.2 presents a functional diagram that illustrates the aeroelastic interaction of these structural and aerodynamic forces.

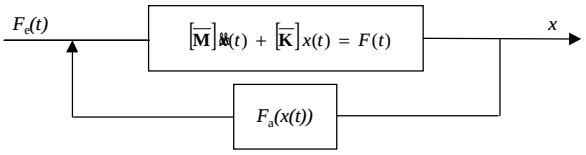

Fig 2. Aeroelastic Functional Diagram

Without the aerodynamic feedback, Fig.2 reduces to an open-loop forced-structural vibration system whose response amplitude is

usually finite. With the inclusion of $\mathbf{F}_a(\mathbf{x})$, Fig.2 represents a closed-loop dynamic response problem which can be expressed by the following equation:

$$\overline{\mathbf{M}}\ddot{\mathbf{x}}(t) + \overline{\mathbf{K}}\mathbf{x}(t) - \mathbf{F}_a(\mathbf{x}) = \mathbf{F}_e(t) \quad (8)$$

Eq(8) is obtained by combining Eq(6) and Eq(7). The left hand side of Eq(8) is in fact a closed-loop dynamic system which can be self-excited in nature. This gives rise to a stability problem of the closed-loop dynamic system known as flutter. Flutter analysis usually involves the search of the structural stability boundary of an aircraft structure in terms of its flight speed and altitude or the corresponding dynamic pressure. If $\mathbf{F}_a(\mathbf{x})$ is a nonlinear function with respect to $\mathbf{x}(t)$, the flutter analysis must be performed by a time-marching procedure solving the following equation:

$$\overline{\mathbf{M}}\ddot{\mathbf{x}}(t) + \overline{\mathbf{K}}\mathbf{x}(t) - \mathbf{F}_a(\mathbf{x}) = 0 \quad (9)$$

with initial condition of $\mathbf{x}(0)$ and $\dot{\mathbf{x}}(0)$ being specified at $t = 0$.

In this paper, aeroelastic analysis was adopted by commercial software MSC Nastran.

4. Structure model

A half model of a aircraft with an elastic wing was employed and Fig.3 is its structural view. The length of the model was 3.36m. Fig.4 presents mesh generation by ICEM CFD. Total elements were 18,753,668. Due to the large amount of elements, numerical simulation was completed by a computer cluster with 128 Cpus, as shown in Fig.5.

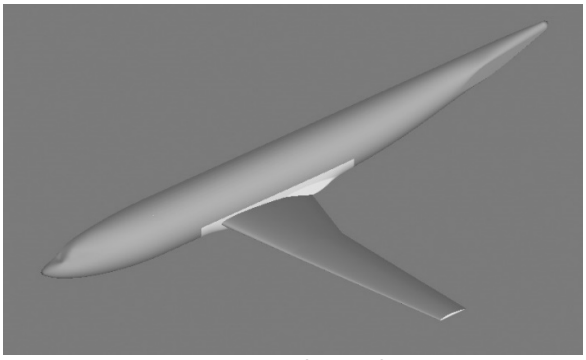

Fig 3. Structure view of a half model with an elastic wing.

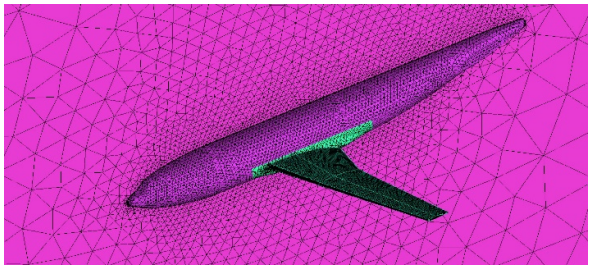

Fig 4. Mesh generation

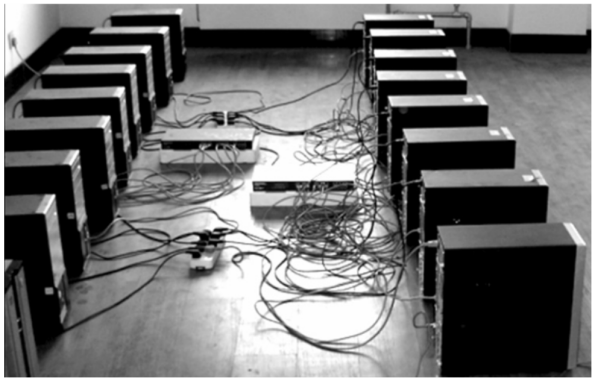

Fig 5. Computer cluster

5. Scaled model computation

Scaled model parameters were prepared and computed by the following algorithm:

Scaled ratios K_l ; dynamic pressure ratio K_q ; density ratio K_r ; Stiffness ratio $\mathrm{K_{EI}} = \mathrm{K_q} K_l^4$; mass ratio $K_m = K_r K_l^3$; frequency ratio $K_f = K_q^{\frac{1}{2}} K_r^{-\frac{1}{2}} K_l^{-1}$

In the present paper, three kinds of length of the model was investigated. The base length of the rhomboid zone is 2.15m without arrangement requirement length. With a scaled ratio 1.5, the exceed range is 1.5%; with a scaled ratio 1.49, the exceed range is 5%; and with a scaled ratio 1.42, the exceed range is 10%. Based on the three type scales ratio, the other scaled parameters can be established.

6. Result and Discussion

6.1 Aerodynamic force

With Mach number is 3, tabel 1 presents lift force coefficients of the wing for the three exceed range based on CFD computation. It can be seen

that: for the two exceed range (i.e. 1.5% and 5%), the influence was able to be neglected; and the other ranges 10% was not able to be neglected.

Table 1 Lift force comparison

Angle of attack (°)	Exceed range		
	1.5%	5%	10%
-4	-0.0043	-0.0042	-0.0074
-2	-0.0021	-0.0021	-0.0058
0	0.0006	0.0006	0.0007
2	0.0027	0.0027	0.0061
4	0.0046	0.0046	0.0079

6.2 Aeroelasticity

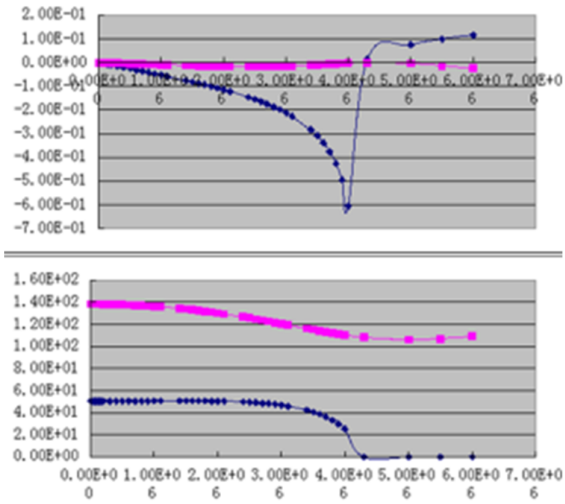

Fig 6. V-g and V-f view of the exceed range 1.5%

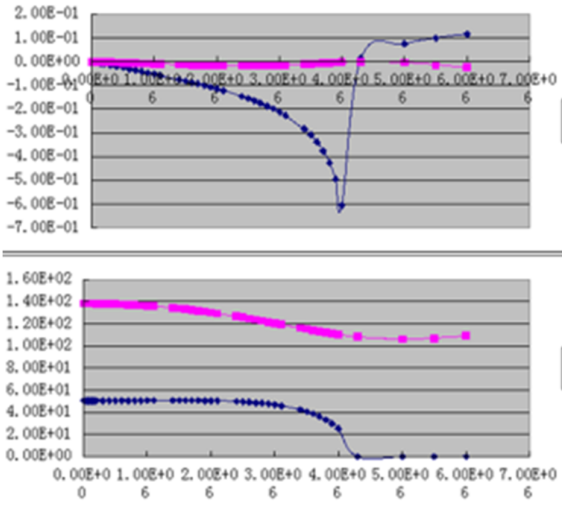

Fig 7. V-g and V-f view of the exceed range 5%

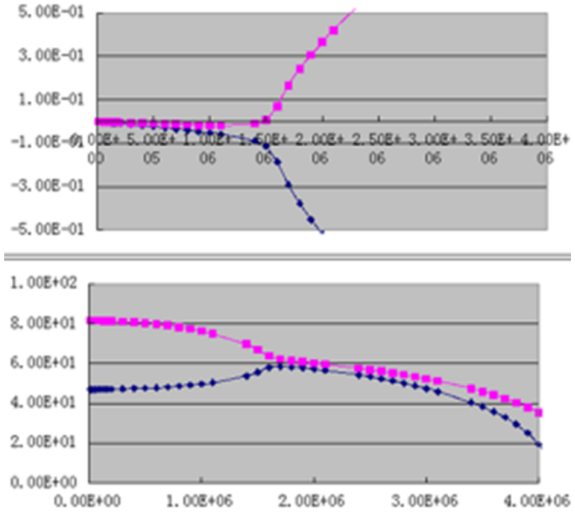

Fig 8. V-g and V-f view of the exceed range 10%

For the different scaled ratio, V-g and V-f relationships were computed, as shown in Figs.6-8. It can be seen that: for the two exceed range (i.e. 1.5% and 5%), the influence was able to be neglected; and the other ranges 10% was not able to be neglected.

The influence due to rhomboid zone of the present wind tunnel can be improved with two ways: the first way is to reduce the size of the model into the range of rhomboid zone with proper scaled ratio; the other way is to modify the wind tunnel wall curve with mechanical control.

7. Conclusions

In this paper, influence of three different exceed range on rhomboid zone of a Chinese wind tunnel was investigated. The results proposed that if exceed range was increased, the aeroelastic wind tunnel test results will be influenced obviously.

In order to find believable experimental results, the scaled model is better to arranged inside the rhomboid zone. In some special condition due to the limit of the scaled parameters, the influence of the exceed range must be predicted before wind tunnel tests and the model production.

8. Reference

[1] Shen A. Optimization of energy extraction in transverse galloping. J*ournal of Fluids & Structures*, 2013, 43(7):124–144.
[2] Cunningham M J. Hypersonic aerodynamics for an entry research vehicle. *Journal of Spacecraft & Rockets*, 2015, 24(2):97-98.
[3] Bai Y G, Sun D K, Lin J H. Three dimensional numerical simulations of long-span bridge aerodynamics, using block-iterative coupling and DES. *Computers & Fluids*, 2010, 39(9): 1549-1561
[4] Albano E and Rodden W P. A doublet-lattice method for calculating lift distributions on oscillating surfaces in subsonic flows. *AIAA Journal*, 1969, 7: 279-285

Copyright Statement

Contact Author Email Address

Name: Mr. Yuguang Bai, Doctor/Lecturer
Address: 2 Linggong Road, Ganjingzi District, School of Aeronautics and Astronautics, Dalian University of Technology Dalian 116023, China
E-mail: baiyg@dlut.edu.cn
Tel: 86 (0) 15668691118 (mobile)
86 411 84706213 (office)